Some applications of L^∞ constraints in image processing

Pierre WEISS

Advisors : Laure Blanc-Féraud, Gilles Aubert

September 15, 2006

Introduction

The framework

Many image restoration or decomposition algorithms are formulated as an optimization process :

$$\inf_u \{J(u) + \lambda K(u, u_0)\}$$

Where :

- J is a convex regularization functional.
- K is a convex data term functional.
- The functionals are often a mixture of L^p norms.

Notations

- $||u||_{l^p} = (\sum_i |u_i|_2^p)^{1/p}$
- $||u||_{L^\infty} = \max_i(|u_i|_2)$
- $TV(u) = J_1(u) = \sum_i |(\nabla u)_i|_2$

Some examples

- Gaussian convolution :

$$\inf_u \{||(|\nabla u|)||_{L^2}^2 + \lambda ||u - u_0||_{L^2}^2\}$$

- Rudin-Osher-Fatemi or $BV - L^2$ model :

$$\inf_u \{TV(u) + \lambda ||u - u_0||_{L^2}^2\}$$

- $BV - L^1$ model (Alliney, Nikolova, Chan, Darbon,...) :

$$\inf_u \{TV(u) + \lambda ||u - u_0||_{L^1}\}$$

Introduction

The L^∞-norm appears naturally

- Bounded noise.
- Y. Meyer's decomposition.
- Morel and al's axiomatic approach for image inpainting.

Though it is fewly used

- Convex but not strictly convex functional $\longrightarrow$ non uniqueness of the solutions.
- As the L^1 norm, more difficult to handle numerically than L^2 or L^p norms.

$\longrightarrow$ **Aim of our work :** exploit this norm for some tasks of image processing.

General problem

In this talk, we focus on the following problem :

$$\inf_{u \in K} J(u) \tag{1}$$

with K defined as :

$$K = \{u \in Z, ||u - f||_\infty \leq \alpha\} \tag{2}$$

$Z = \mathbb{R}^n$ (space of images with $n = n_x n_y$) or $Z = \mathbb{R}^n \times \mathbb{R}^2$ (space of vector fields).

$\rightarrow$ In general, the solution is not unique.

Introduction

Outline of the talk

1. A convergent algorithm : the projected subgradient descent.
2. Application to Y. Meyer's model.
3. Application to $BV - L^p$ problems.
4. Application to bounded noises denoising.

Algorithmic considerations

Complexity of the problem

Objective find $\bar{u}$ such that :

$$\bar{u} = arginf_{u \in K} J(u) \tag{3}$$

- J convex.
- K compact, convex set.

Algorithmic considerations

Complexity of the problem

Objective find $\bar{u}$ such that :

$$\bar{u} = arginf_{u \in K} J(u) \tag{3}$$

- J convex.
- K compact, convex set.

Recall : the subdifferential of J at point u is defined by :

$$\partial J(u) = \{\eta, J(u) + < \eta, (x - u) >_Z \leq J(x)\} \tag{4}$$

Algorithmic considerations

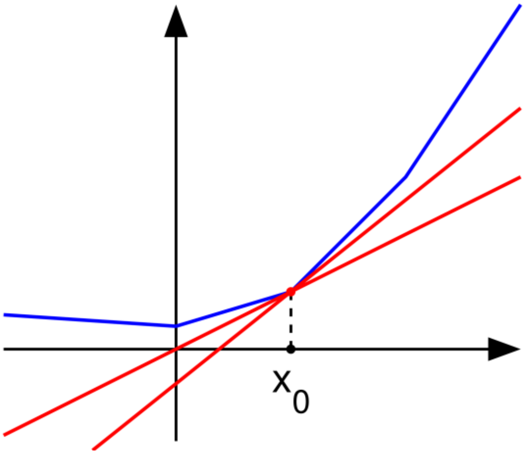

Algorithmic considerations

Complexity of the problem

An algorithm generates :

- A sequence $\{u^k\}$ that is suppose to approach $\bar{u}$.
- An associated sequence of subgradients $\partial J(u^k)$ and of values $J(u^k)$.
- At iteration k : $\bar{J}^k = \min_{i\in\{1,\dots,k\}} J(u^k)$

Algorithmic considerations

Complexity of the problem

An algorithm generates :

- A sequence $\{u^k\}$ that is suppose to approach $\bar{u}$.
- An associated sequence of subgradients $\partial J(u^k)$ and of values $J(u^k)$.
- At iteration k : $\bar{J}^k = \min_{i\in\{1,\dots,k\}} J(u^k)$

To have $|\bar{J}^k - \bar{J}| \leq \epsilon$ we need $k \geq \lfloor \frac{C}{\epsilon^2} \rfloor$

Algorithmic considerations

An optimal algorithm

The projected subgradient descent is the following process :

$$\begin{cases} u^0 \in K \\ u^{k+1} = \Pi_K(u^k - t_k \frac{\eta^k}{||\eta^k||_2}) \end{cases} \tag{5}$$

Here, $t_k > 0$ for any k, η^k is any element of $\partial J(u^k)$.

Conditions of applicability

For efficiency of this method :

- Π_K must be computable easily.
- We need to be able to compute subgradients.

Algorithmic considerations

An optimal algorithm

If J is Lipschitz continuous :

$$|J(u) - J(v)| \leq L||u - v||_2 \tag{6}$$

we can find a parameterless optimal sequence.
The projected subgradient descent with step :

$$t_k = \frac{D}{\sqrt{k}} \tag{7}$$

ensures that :

$$\epsilon_k = \bar{J}^k - \bar{J} \leq O(1)\frac{LD}{\sqrt{k}} \tag{8}$$

where D is the Euclidean diameter of the set K.

Algorithmic considerations

An optimal algorithm

If ∇J is Lipschitz continuous :

$$||\nabla J(u) - \nabla J(v)||_2 \leq L' ||u - v||_2 \tag{9}$$

then the projected gradient descent :

$$\begin{cases} u^0 \in K \\ u^{k+1} = \Pi_K(u^k - t\nabla J(u^k)) \end{cases} \tag{10}$$

with constant step $t = \frac{2}{L'}$ ensures that :

$$d(u^k, U_0) \to 0 \tag{11}$$

A new numerical solution to Y. Meyer's model

The idea of Y. Meyer

Decompose an image in two components $f = u + v$.

- u contains the geometry
- v contains texture and or noise

The G norm and the model

Decomposition model :

$$\inf_{u \in BV(\Omega), v \in G, f=u+v} \left\{ \int_\Omega |Du| + \lambda ||v||_G \right\}$$

With :

$$||v||_G = \inf_g \{ ||g||_\infty, div(g) = v, g = (g_1, g_2), |g| = \sqrt{g_1^2 + g_2^2} \}$$

A new numerical solution to Y. Meyer's model

The G norm and the model

Decomposition model :

$$\inf_{u \in BV(\Omega), v \in G, f=u+v} \{ \int_{\Omega} |Du| + \lambda ||v||_G \}$$

With :

$$||v||_G = \inf_g \{ ||g||_{\infty}, div(g) = v, g = (g_1, g_2), |g| = \sqrt{g_1^2 + g_2^2} \}$$

Definition and properties

If $f_n \rightharpoonup 0$ then $||f_n||_G \to 0$

- $||sin(nx)||_{L^2([0,2\pi])} = \pi \quad \forall n \in \mathbb{N}$
- $||sin(nx)||_{G([0,2\pi])} = 1/n \quad \forall n \in \mathbb{N}$

A new simple method

Use the **change of variable** $u = f - div(g)$.

$\longrightarrow$ Avoids the need of a penalty optimization method to impose $f = u + v$.

$$\begin{aligned} & \inf_u \{ TV(u) + \lambda \inf_g \{ ||g||_\infty, div(g) = f - u \} \} \\ = \; & \inf_g \{ TV(f - div(g)) + \lambda ||g||_\infty \} \end{aligned}$$

Y. Meyer's problem is thus reformulated as :

$$\inf_{g, ||g||_\infty \leq \alpha} \{ TV(f - div(g)) \}$$

Numerical details :

If $J(g) = TV(f - div(g))$, one element η of $\partial J(g)$ is given by :

$$\eta = -\nabla div(\Psi) \tag{12}$$

with :

$$(\Psi)_i = \begin{cases} \frac{(\nabla(f-div(g))_i}{|(\nabla(f-div(g))_i|_2} & \text{if } |(\nabla(f-div(g))_i|_2 > 0 \\ 0 & \text{otherwise} \end{cases} \tag{13}$$

Numerical details :

The diameter of K is :

$$D = 2\alpha\sqrt{n} \tag{14}$$

J is L-Lipschitz with :

$$L \leq 16\sqrt{n} \tag{15}$$

The complexity of the projected subgradient descent is thus :

$$O(1)\frac{16\alpha n}{\sqrt{k}} \tag{16}$$

It increases linearly with α and n.

After 4 seconds (100 iterations)

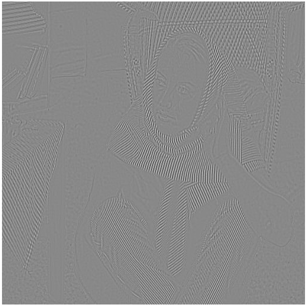

After 5 minutes (7500 iterations)

$BV - l^p$ models

The problem

We now focus on :

$$\inf_u \lambda |u - f|_p^p + TV(u) \tag{17}$$

for $p \in [1, \infty[$.

- When $p = 2$, we get Rudin, Osher, Fatemi model.
- When $p = 1$, we get $BV - L^1$ model.

This problem is difficult, due to the non differentiability of TV.

$BV - l^p$ models

Results of duality

For $p \in]1, \infty[$, the dual problem is defined by :

$$\inf_{\{q \in Y, ||q||_\infty \leq 1\}} < -div(q), f >_X - \beta |div(q)|_{p'}^{p'} \tag{18}$$

The extremality relations lead to :

$$\bar{u} = f - \beta p' |div(q)|^{p'-2} div(\bar{q}) \tag{19}$$

$\rightarrow$ We can use a constant step projected gradient descent to solve (18). In practice computation times decrease!

$BV - L^1$ model and duality

The dual problem of the $BV - L^1$ problem is given by :

$$\inf_{\{q \in Y, ||q||_\infty \leq 1\}} < -div(q), f >_X + \lambda |div(q)|_\infty \tag{20}$$

The first extremality relations leads to :

$$(\nabla \bar{u})_i = |(\nabla \bar{u})_i|_2 \bar{q}_i \tag{21}$$

$\Rightarrow$ $\bar{q}$ represents the orientation of the level lines of $\bar{u}$.

$BV - L^1$ model and duality

The second extremality relation leads to :

$$\bar{u}_i = f_i + \lambda \gamma_i \frac{(-div(\bar{q}))_i}{|(div(\bar{q}))_i|} \tag{22}$$

With $\gamma = (\gamma_1, \gamma_2, ..., \gamma_n) \in \mathbb{R}^n$ such that :

$$\left\{ \begin{array}{rcl} \gamma_i & \geq & 0 \;\; \forall i \in \{1, 2, ..., n\} \\ |\gamma|_1 & = & 1 \\ \gamma_i & = & 0 \text{ if } |(div(\bar{q}))_i| < |div(\bar{q})|_\infty \end{array} \right. \tag{23}$$

$\Rightarrow$ Many pixels remain unchanged!

$BV - L^1$ model and duality

The second extremality relation leads to :

$$\bar{u}_i = f_i + \lambda \gamma_i \frac{(-div(\bar{q}))_i}{|(div(\bar{q}))_i|} \tag{22}$$

With $\gamma = (\gamma_1, \gamma_2, ..., \gamma_n) \in \mathbb{R}^n$ such that :

$$\left\{ \begin{array}{lll} \gamma_i & \geq & 0 \quad \forall i \in \{1, 2, ..., n\} \\ |\gamma|_1 & = & 1 \\ \gamma_i & = & 0 \text{ if } |(div(\bar{q}))_i| < |div(\bar{q})|_\infty \end{array} \right. \tag{23}$$

$\Rightarrow$ Many pixels remain unchanged!

$\rightarrow$ But, numerical interest seems limited.

The models studied

In this last part, we focus on two models. The first is :

$$\inf_{\{u, |u-f|_\infty \leq \alpha\}} TV(u) \tag{24}$$

The second is the discretized hypersurface of u :

$$\inf_{\{u, |u-f|_\infty \leq \alpha\}} J_2(u) \tag{25}$$

$J_2(u)$ is the discretized hypersurface of u :

$$J_2(u) := \sum_{i=1}^{n} \sqrt{|\nabla u|_2^2 + 1} \tag{26}$$

Uniform white noise a first justification

If $f = u + b$, with $b \sim U([-\alpha, \alpha])$.

If we have a probability on the images $P(u) = C\exp(-J(u))$.

Then the Maximum a posteriori (MAP) solution is given by :

$$\inf_{\{u, |u-f|_\infty \leq \alpha\}} J(u) \tag{27}$$

Quantization a second justification

If Q is the 2α quantization operator :

$$\begin{array}{rcccl} Q & : & \mathbb{R} & \rightarrow & 2\alpha\mathbb{N} \\ & & u_i & \rightarrow & 2\alpha\lfloor\frac{u}{2\alpha}\rfloor + \alpha \end{array} \quad (28)$$

Then :

$$Q^{-1}(f) = \{u, f = Q(u)\} = \{u, |u - f|_\infty \leq \alpha\} \quad (29)$$

We can look for the solution of maximal probability in $Q^{-1}(f)$.

Uniqueness of the solution

The solution of $J_2 - L^\infty$ is generally unique. The solution of $BV - L^\infty$ is not.

$$\inf_{u, ||u_0 - u||_\infty \leq \alpha} \left\{ \int_\Omega |\nabla u| dx \right\}$$

An example : $u_0 = x$ on $[0, 1]$.

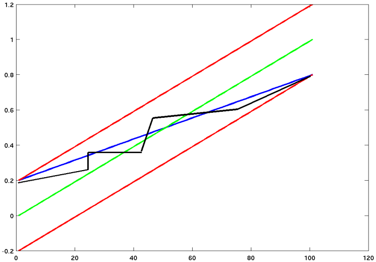

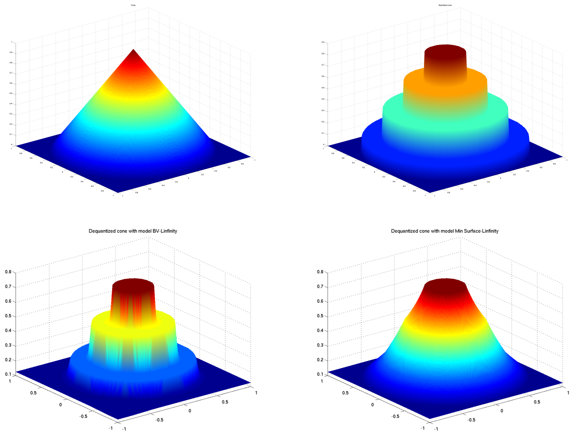
Dequantized cone with model BV-Linfinity
Dequantized cone with model Min Surface-Linfinity
0.8
0.7
0.6
0.5
0.4
0.3
0.2
0.1
1
0.5
0
-0.5
-1

$BV - L^\infty$ and $MinSurface - L^\infty$ on a quantized image

$BV - L^\infty$ and $MinSurface - L^\infty$ on a noisy image

Conclusion

Summary

- Proposed a general framework for l^∞ constraints.
- Showed that the projected subgradient is a really efficient scheme for :
  1. Y. Meyer's problem.
  2. $BV - l^p$ problems.
  3. Denoising of bounded noises.

Conclusion

Summary

- Proposed a general framework for l^∞ constraints.
- Showed that the projected subgradient is a really efficient scheme for :
  1. Y. Meyer's problem.
  2. $BV - l^p$ problems.
  3. Denoising of bounded noises.

Future...

- Deeper analysis of Y. Meyer's model, to explain its witnessed weaknesses.
- Faster algorithms, based on specific properties of the functions used.

Thanks a lot for your attention!

How does Meyer's model react to different frequencies?

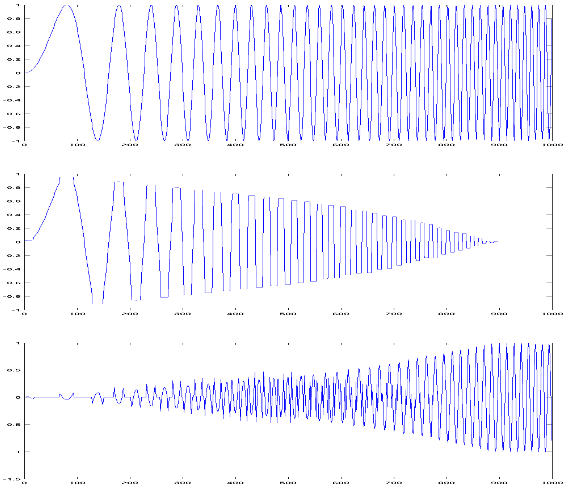

Figure: Top : initial function $\sin(\gamma x^2)$, Middle : geometrical part given by Y. Meyer's model, bottom : oscillating part

Comparison of different norms

Experimental tests by J.F. Aujol

Norms / Image	Geometric	Textured	Noise
TV	64 600	1 000 000	2 100 000
L^2	9 500	9 500	9 500
G	2 000	360	120